FEBS Letters 586 (2012) 416–421

journal homepage: www.FEBSLetters.org

Single-particle tracking of immunoglobulin E receptors (FcεRI) in micron-sized clusters and receptor patches

Kathrin Spendier [a,b], Keith A. Lidke [a], Diane S. Lidke [c], James L. Thomas [a,*]

[a] Department of Physics and Astronomy, University of New Mexico, Albuquerque, NM 87131, USA
[b] Consortium of the Americas for Interdisciplinary Science, University of New Mexico, Albuquerque, NM 87131, USA
[c] Department of Pathology and Cancer Research and Treatment Center, University of New Mexico, Albuquerque, NM 87131, USA

ARTICLE INFO

Article history:
Received 22 December 2011
Revised 4 January 2012
Accepted 9 January 2012
Available online 18 January 2012

Edited by Sandro Sonnino

Keywords:
FcεRI
Mast cell
Single-particle tracking
Supported lipid bilayer
TIRF microscopy
Monte Carlo calculation

ABSTRACT

When mast cells contact a monovalent antigen-bearing fluid lipid bilayer, IgE-loaded FcεRI receptors aggregate at contact points and trigger degranulation and the release of immune activators. We used two-color total internal reflection fluorescence microscopy and single-particle tracking to show that most fluorescently labeled receptor complexes diffuse freely within these micron-size clusters, with a diffusion coefficient comparable to free receptors in resting cells. At later times, when the small clusters coalesce to form larger patches, receptors diffuse even more rapidly. In all cases, Monte Carlo diffusion simulations ensured that the tracking results were free of bias, and distinguished biological from statistical variation. These results show the diversity in receptor mobility in mast cells, demonstrating at least three distinct states of receptor diffusivity.

1. Introduction

Mast cells are immune cells found in tissues throughout the body, including the skin and mucosal surfaces. When activated, they protect the body from parasitic infections, but are also responsible for allergic responses. In mast cells and basophils, a crucial player in this process is the high affinity immunoglobulin E (IgE) receptor (FcεRI). In allergic responses, multivalent ligand, e.g. a pollen grain, binds to IgE-loaded receptors (IgE–FcεRI) causing receptor aggregation also known as receptor cross-linking. Aggregation of these transmembrane receptors leads to receptor phosphorylation [1,2] and the subsequent initiation of signaling cascades that result in the release of inflammatory mediators such as histamine and serotonin [2].

To study immune signaling by mast cells, the rat basophilic leukemia 2H3 (RBL) cell line is typically used as a model [3–5]. In previous studies, it was observed that RBL cells loaded with fluorescent IgE form receptor aggregates when allowed to settle under gravity [6,7], or when pipette-pressed [8], onto fluid bilayers containing monovalent ligands. These receptor aggregates are not cross-linked and hence are different in character from clusters formed by multivalent ligands. However, RBL cell signaling still occurs on these fluid lipid membrane substrates [6,7]. Our recent work [8] showed that receptor clusters on ligand-presenting fluid bilayers originate from cell surface protrusions that form the initial contact points with the substrate. Receptor accumulation at these contact points was shown to be kinetically consistent with diffusion limited trapping; moreover, the cell membrane was far from the substrate *except* at receptor clusters, as shown by a dye exclusion study. After initial IgE–FcεRI cluster formation, small clusters diffuse slowly and coalesce to form a large central patch, termed the mast cell synapse, in which IgE–FcεRI were qualitatively observed to be laterally mobile [7]. The ability of monovalent ligands presented on fluid membranes to stimulate RBL cells speaks to a longstanding debate on the relationship between IgE–FcεRI mobility and signaling. Recently, it has been demonstrated that small antigen-induced IgE–FcεRI clusters can induce signaling while retaining mobility [9]. The principal aim of this paper is to quantify the mobility of IgE–FcεRI within initial cell–substrate contact points (receptor clusters), and in the larger patches, in order to address the role of IgE–FcεRI mobility in RBL cell activation and more fully characterize the diffusional behavior of this receptor.

Because the receptor clusters are typically smaller than a micron, methods such as photobleaching recovery or far-field fluorescence correlation spectroscopy are ill-suited for measuring receptor diffusion. Instead, we have turned to single-particle tracking, using the fluorescent dye Atto647, which yielded receptor

* Corresponding author. Fax: +1 505 277 1520.
E-mail address: jthomas@unm.edu (J.L. Thomas).

0014-5793/$36.00
doi:10.1016/j.febslet.2012.01.013

trajectories with ca. 50 nm localization precision. To ensure that tracked receptors were in clusters, the majority of the receptor complexes were labeled with Alexa488; both dyes were imaged using a two-color total internal reflection fluorescence (TIRF) microscope. Analysis of single-particle trajectories showed that receptors maintain their diffusivity even when confined within receptor clusters, and increase their diffusivity (above that of monomeric unliganded IgE–FcεRI) in central patches. Together with the observation that weak signaling occurs when FcεRI on mast cells is presented with mobile, bilayer-incorporated ligand [7], this study shows clearly that signaling occurs under conditions where a majority of receptors (~70%) remain mobile.

2. Materials and methods

2.1. Two color labeling of RBL Cells

RBL-2H3 cells were maintained in Minimal Essential Medium (MEM) (Invitrogen) with 10% Fetal Calf Serum. At the day of the experiment, MEM with Fetal Calf Serum was exchanged with MEM supplemented with 10% Fetal Bovine Serum, 1% Penicillin–Streptomycin, and 1% L-glutamine, which will be referred to as media in the remainder of this manuscript. Anti-DNP IgE was purified as previously described [10,11]. Fluorescent anti-DNP IgE conjugates were created using Alexa488 (Invitrogen) and Atto647 (ATTO-TEC GmbH). Prior to microscopy, cells were fluorescent IgE primed by first incubating with 35 or 50 pM Atto647-IgE anti-DNP in media for 10 min at 37 °C and then washed 5 times with 2 ml media obtaining a final aliquot of 2 ml. Next 5 μl of Alexa488-IgE anti-DNP at a concentration of 0.7 μg/ml was added and incubated for 10 min at 37 °C. The primed cells with both fluorescent markers were then washed 4 times with 2 ml media and divided into 0.5 ml aliquots (~50 000 cells per aliquot) stored in 1 ml tubes at 37 °C in a humidified chamber with 5% CO_2 until later use.

2.2. Supported lipid bilayers

Prior to use, microscope glass cover slips were cleaned of organic residues with a mixture of sulfuric acid and hydrogen peroxide (“piranha” solution). Supported lipid bilayers [7] were made by spontaneous liposome fusion [12]. Lipids (Avanti) were dissolved in chloroform, dried under N_2, and then placed under vacuum for 1 h. The lipid film was then suspended in PBS + 2 mM Mg^{2+} to 1.3 mM and sonicated for 5 min using a probe sonicator. Laterally mobile bilayers were formed from 1-palmitoyl-2-oleoyl-*sn*-glycero-3-phosphocholine (POPC) and 12 mol% *N*-dinitrophenyl-aminocaproyl phosphatidylethanolamine (DNP-Cap PE) on piranha-cleaned cover glass for 15 min on a slide warmer at 37 °C. Each bilayer coated coverslip was kept immersed during transfer to the imaging chamber. Prior to adding cells to the bilayer, the chamber was flushed with 500 μl of media. Lipid mobility was checked using single-particle tracking as described elsewhere [7].

2.3. Fluorescence microscopy

Objective-based total internal reflection fluorescent microscopy was performed on an Olympus IX 71 (Olympus America Inc.) inverted microscope with a 150 × 1.45 NA oil objective using a 472 nm laser (CrystaLaser) to excite Alexa488 and a 635 nm laser (Coherent Inc.) to excite Atto647 with an evanescent wave. Two-color fluorescent images were collected at a frame rate of 20 frames/s using an electron multiplying CCD camera (Andor iXon + 897; Andor Technologies Inc.) and spectrally separated by an image splitter (Quad-View™, Optical Insights, LLC). The camera was cooled to −70 °C with a detector gain of 200. Sample temperatures were maintained at ~37 °C with an objective heater (Bioptechs Inc.) and images were collected with in-house software implemented in MATLAB (The MathWorks Inc.). Images were processed using MATLAB in conjunction with DIPImage [13], an image processing library. Two-color fluorescent images were collected in two channels. The red channel recorded the lower concentration of Atto647-IgE in the single-particle regime. Images in the green channel (Alexa488) recorded the fluorescent label of higher concentration to outline the spatial extent of receptor clusters and central patches. To overlay these two channels a dilute sample of 0.1 μm diameter fluorescent microspheres (yellow/green FluoSpheres, Molecular Probes Inc.) emitting spectral components detectable in both channels was imaged. The images of these microspheres were used to align the two channels.

2.4. Single-particle tracking

Single-particle trajectories of fluorescent receptor clusters and IgE–FcεRI receptor complexes were obtained by using a single-particle tracking algorithm implemented in MATLAB as previously described in Ref. [14]. IgE–FcεRI were tracked only if they were located within a receptor cluster or a central patch as determined from the two-color image overlay. The particles were tracked in a 50 ms time interval for at least 65 time steps. The average track length was ~100 time steps. The mean-squared displacement (MSD) was calculated from all n available displacements of a given duration $n\Delta t$ in the track record [15–17]. To characterize the motion, the MSD plot was computed up to Δt<1/4 of the total number of acquired time frames [16,18]. The MSD graph for IgE–FcεRI inside receptor clusters and in the central patch showed a downward curvature and asymptotically approached a finite value, which is a signature for confined diffusion. As the exact shape of the confinement (if it is not too eccentric) has a negligible effect on the form of the MSD [19], we fit to a circular confinement zone. The exact solution [20] contains an infinite sum of exponentials, but the second term is two orders of magnitude smaller than the first (and each subsequent term at least another order of magnitude smaller), so that a good approximation is obtained from the first exponential only:

$$\mathrm{MSD}(\Delta t) = 4\sigma^2 + R^2[1 - 0.99\exp(-3.393D\Delta t/R^2)].$$

Fitting parameter D is the diffusion coefficient and R is the confinement zone radius. σ is the sum of the static and dynamic localization (measurement) uncertainty [17,21], determined by fitting a straight line through time lags $2\Delta t$, $3\Delta t$, and $4\Delta t$. The offset determined by this method avoids using the part of the MSD plot between times 0 and $2\Delta t$ which is known to be complicated and times longer than $4\Delta t$ after which the confinement effects were apparent [22]. The average localization uncertainty for IgE–FcεRI diffusing inside clusters and central patches was $\sigma = 47 \pm 18$ and 30 ± 38 nm, respectively, where the error represents one standard deviation.

Cluster diffusion was also estimated from MSD plots of the cluster center, as determined from a 2D Gaussian fit to intensity. The MSD graph of receptor cluster trajectories was linear and fit to $\mathrm{MSD}(\Delta t) = 4\sigma^2 + 4D\Delta t$ to estimate cluster diffusivity. The average localization uncertainty for clusters was $\sigma = 32 \pm 13$ nm. In MSD plots, all points were equally weighted, which has been shown to give unbiased parameters if all available displacements are used [16,17].

2.5. Monte Carlo calculations

To determine statistical uncertainties (and possible biases) in fitting for diffusivity, model diffusion tracks were constructed

using a random-step-length continuum algorithm, and the tracks were analyzed with same procedure employed for cell data. A point particle was initially placed at a random position within a circular domain of radius R. At each time step, the particle was moved a displacement $\gamma\sqrt{2Dt}$ in x and y, where t is the time step, D the diffusion coefficient, and γ is a normally distributed pseudo-random number with zero mean and unit standard deviation. When a particle attempted to cross the boundary, its trajectory was reflected by the boundary resulting in confined diffusion. To simulate simple diffusion we applied the same algorithm in the absence of a reflecting boundary. The final simulated real particle trajectory (without localization uncertainty) contained 100 position measurements. To obtain an experimentally observed particle trajectory a dynamic and static localization uncertainty must be added. Static errors arise from the uncertainty in determining the position of the particle due to experimental noise. Dynamic errors are due to particle diffusion within the integration time of each frame, leading to intensity blurring. Both sources of error have a Gaussian distribution and can be combined into one parameter $\gamma\sigma$ which was added to each x and y coordinates of the trajectory.

The simulation was repeated 50 000 times for each initial Monte Carlo diffusion coefficient D and corral radius R. D_{fit} and R_{fit} obtained from the fits to the MSD plots were nearly lognormally distributed, see supplemental Fig. S1; such a distribution of diffusivities has been reported for unconfined diffusion as well [16,23]. Accordingly, we characterize the distribution by the (exponential of the) mean log diffusivity $\langle D_0\rangle_{\ln}$ and corral radius $\langle R_0\rangle_{\ln}$, and the corresponding standard deviations. Note that in lognormal distributions, the standard deviation represents a multiplicative (rather than additive) uncertainty. To simplify notation, in the remainder of this manuscript we will drop the subscript "ln" and use the averaging brackets to denote the logarithmic mean, and $\times/$ to indicate the multiplicative uncertainty. It is also worth noting that many studies of diffusion on cells report uncertainties as the standard error or the mean (or of the log mean), which is much smaller than the full spread in the distribution of measurements, reported here.

Monte Carlo simulations were performed in MATLAB. The MATLAB code is available in the supplemental material.

3. Results and discussion

3.1. IgE–FcεRI receptors maintain lateral mobility in micron-sized receptor clusters and central patches

To investigate if individual IgE–FcεRI complexes are laterally mobile within receptor clusters and central patches a two-color fluorescent experiment was performed as outlined in Section 2. Fluorescent IgE-loaded RBL cells were allowed to settle under gravity onto fluid lipid bilayers that contained 12 mol% DNP-CAP PE lipid. TIRF microscopy using simultaneous 472 and 635 nm laser illumination was used to image fluorescent structures within ~200 nm of the cell–substrate interface. Microscope time series of 50 s (1000 frames) were collected after ~30 s and ~4 min of initial cell–substrate contact. Receptor motion in clusters and central patches were investigated at early and late time points, respectively. After spatially overlaying the two spectrally separated time series, the majority of IgE–FcεRI was observed to be mobile within clusters and central patches as shown in *supplementary* movies S1 and S2, respectively.

In a recent study [7] our group showed that individual IgE–FcεRI was mobile within a central patch by a fluorescent bleaching and recovery experiment. However, the collected experimental data did not allow us to estimate the receptor diffusion coefficient. To make quantitative measurements of receptor motion within clusters and central patches the method of single-particle tracking [14,21] was applied here.

Fig. 1B and E depict typical IgE–FcεRI trajectories (red) imaged at 20 frames/s within a cluster (green) and a central patch (green), respectively. Corresponding MSD plots depicted in Fig. 1C (circles) and F showed downward curvature and asymptotically approached a finite value, which is a signature for confined diffusion. This functional form was expected since it is evident from Fig. 1B and E that receptor trajectories were confined within the cluster and central patch. Moreover, the much steeper initial slope of the MSD for the receptor in the patch (Fig. 1F) compared to that for the receptor in the small cluster (Fig. 1C, circles) shows that the former diffuses much faster. To show that receptors are indeed mobile within clusters and eliminate the possibility that the trajectory shown in Fig. 1B (red) describes the actual cluster motion, the cluster was separately tracked. The MSD plot obtained from the cluster trajectory is shown in Fig. 1C (squares); from the linear fit, we find that the diffusion of the cluster as a whole is an order of magnitude slower than that of the individually tracked receptor. (In addition, for a fraction of IgE–FcεRI that had very slow diffusion, we found no directional correlation between receptor hops and cluster hops, vide infra.)

3.2. IgE–FcεRI receptors diffuse fastest in central patches

To quantitatively obtain the receptor diffusion coefficient in clusters and central patches, multiple receptors were tracked on three different cells at early time (~30 s after initial contact) and late time (~4 min after initial contact). For a receptor confined within a cluster, the cluster trajectory was obtained separately. The MSD was calculated for each trajectory and fit to a simple diffusion (cluster tracks) or confined diffusion model (IgE–FcεRI tracks) to estimate diffusivity and domain size as outlined in Section 2.4. For receptors diffusing inside clusters, two clearly distinguishable populations were observed: one diffusing significantly faster than the cluster (Fig. 1C) and the other (~30% of receptor tracks) with a diffusivity comparable to the clusters themselves. The second population will be analyzed separately in a later section. The average (logarithmic mean) diffusion coefficient of IgE–FcεRI in clusters of the first population was $\langle D\rangle = 4.1 \times 10^{-2}$ μm^2/s, with a spread of a factor of 2.03. The IgE–FcεRI diffusivity in clusters is similar to that of the monomeric, uncrosslinked IgE–FcεRI [14,24]. The average cluster radius $\langle R\rangle$ was 206 nm ($\times/1.36$), which is consistent with the microscopically observable cluster size and previous measurements [8]. IgE–FcεRI receptor complexes confined within central patches of apparent average radius $\langle R\rangle = 503$ nm ($\times/1.45$) diffused faster than expected, with an average diffusivity of $\langle D\rangle = 0.17$ μm^2/s ($\times/1.7$). This diffusion coefficient is significantly faster than the measured diffusivity of monomeric IgE–FcεRI on resting cells [14] and consistent with the apparent absence of actin cytoskeleton in this region [7]. It is also consistent with short-timescale diffusion of FcεRI measured with high speed (750 frames/s) single particle tracking [25], and FRAP on cells swollen by hypoosmotic stress [3], where the constraints of the cytoskeleton are removed. Fig. 2 shows the average diffusion coefficient (solid black line) for IgE–FcεRI receptor complexes diffusing within central patches (circles) and clusters (squares). The average diffusivity of clusters (triangles) was $\langle D\rangle = 3.3 \times 10^{-3}$ μm^2/s ($\times/2.1$), significantly smaller than IgE–FcεRI diffusivity and within previously reported observations [8]. Clusters tracked in this experiment did not show evidence of directed motion (as has been previously reported [8]); however, the tracking time was shorter in this study, making detection of directed motion more difficult. For each population, the dashed line above and below the mean represents one standard deviation in the lognormal distribution. To compare the data sets statistically, the two-sample

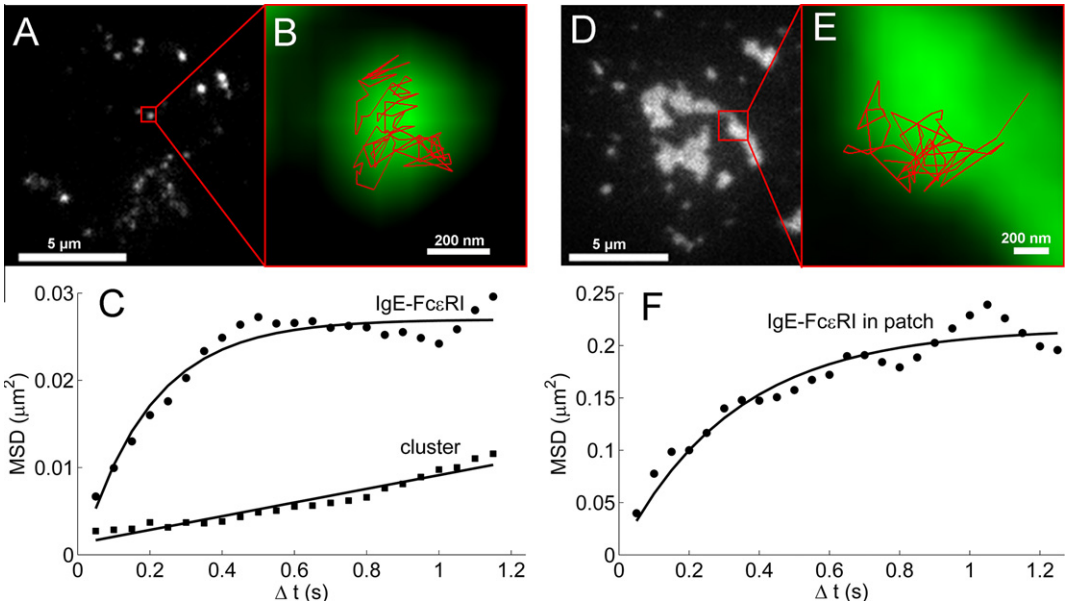

Fig. 1. Fluorescent IgE–FcεRI receptor (IgE–FcεRI) complexes undergo confined diffusion in clusters and central patches. (A and D) Total internal reflection fluorescence microscope image of gravity settling RBL cell on fluid lipid bilayer containing 12 mol% DNP-CAP PE lipid after ~30 s (A) and ~4 min (D) of initial contact. The red box highlights a cluster or central patch in which a single fluorescent IgE–FcεRI complex was tracked at 20 frames/s. Bar = 5 μm. (B) Demonstrates that IgE–FcεRI complex trajectory (red) is restricted to the area occupied by the cluster (green). The cluster image (green) was obtained from an intensity sum over a 4.6 s time series. The cluster moved approximately 140 nm in this time period. (The tracked receptor remained within the patch at all times.) Bar = 200 nm. (C) Mean-squared displacement (MSD) plots of IgE–FcεRI complex trajectory shown in (B) (circles) and cluster trajectory (squares) suggest that IgE–FcεRI diffusivity is an order of magnitude larger than receptor cluster diffusivity. The MSD plot of the tracked IgE–FcεRI complex (circles) indicates confined diffusion by its downward curvature and asymptotic approach to a finite MSD value. From the asymptotic MSD value the estimated circular domain radius is $\sqrt{0.027}$ μm or 160 nm. The MSD plot for the cluster (squares) was linear characterizing simple diffusion. The solid line represents a fit to confined diffusion (circles) or free diffusion (squares). (E) Demonstrates that IgE–FcεRI complex trajectory (red) is restricted to the area occupied by the central patch (green). The patch image (green) was obtained from an intensity sum over a 3.3 s time series. Bar = 200 nm. (F) MSD plot of IgE–FcεRI complex trajectory shown in (E). The IgE–FcεRI complex diffusion was restricted with an estimated circular domain radius of $\sqrt{0.21}$ μm or 460 nm. Moreover, for IgE–FcεRI complexes (circles), the initial slope of the MSD plot in (E) is much stepper than the slope in (C) suggesting that receptor diffuse faster in the central patch than in the cluster.

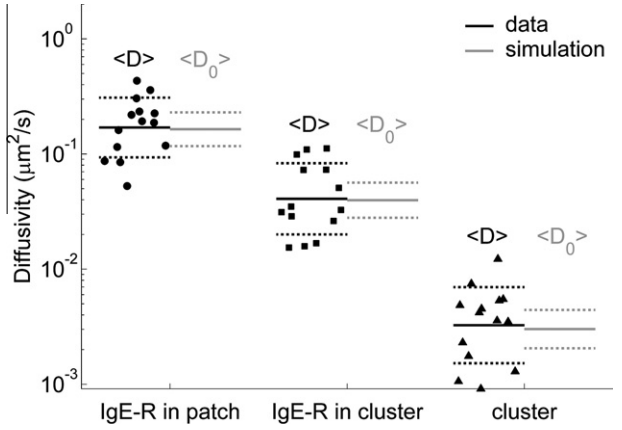

Fig. 2. Experimental (solid black lines) and Monte Carlo simulated (solid gray lines) average (logarithmic mean) diffusivity of IgE–FcεRI receptor complexes confined to central patches (circles) and clusters (squares) as well as average diffusivity of freely diffusing clusters (triangles). For each population, the dashed line above and below the average represents one standard deviation in the lognormal distribution. The average diffusion coefficient $\langle D\rangle$ and corral radius $\langle R\rangle$ obtained from experiments were used as input parameters for the simulation. Here, the averaging brackets denote the logarithmic mean. $\langle D_0\rangle$ is the average diffusivity obtained from 50000 simulations which incorporated dynamic and static localization uncertainty estimated from experimental data. The data presented here suggests that the variation in diffusivity observed on cells (dashed black lines) cannot be explained on the basis of statistics (dashed gray lines). Thus, there is additional variation of *biological* origin.

Kolmogorov–Smirnov test was implemented. This test determined that the three experimental data sets presented in Fig. 2 were drawn from three different distributions at the 5×10^{-4} significance level.

To determine if the variation and uncertainty in diffusivity is consistent with that expected from statistics, Monte Carlo simulations as outlined in Section 2.5 were performed. The experimentally observed average diffusivity $\langle D\rangle$ and corral radius $\langle R\rangle$ (if applicable) for each population were used as simulation input parameters, as well as the localization uncertainty σ. After 50000 Monte Carlo simulations, the population mean and standard deviation of $\langle D_0\rangle$ and $\langle R_0\rangle$ were calculated. The average diffusivity for receptors confined within patches and clusters was $\langle D_0\rangle = 1.6 \times 10^{-1}$ μm²/s (×/1.4) and $\langle D_0\rangle = 4.0 \times 10^{-2}$ μm²/s (×/1.4) with average confinement zone radius of $\langle R_0\rangle = 513$ nm (×/1.3) and $\langle R_0\rangle = 204$ nm (×/1.17), respectively, in good agreement with measured values. This demonstrates that the analysis procedure, with overlapping intervals and equal weighting, does not introduce any substantial bias in parameter estimation, *even in confined diffusion*. (There is evidence of a very small residual bias, which may be caused by the slight deviation of fit D's from a lognormal distribution.)

Monte Carlo simulation of cluster diffusion gave an average diffusivity of $\langle D_0\rangle = 3.0 \times 10^{-3}$ μm²/s (×/1.47), in agreement with the measured value. As discussed above, it has been previously noted that MSD fitting for unconfined diffusion gives unbiased estimates when overlapping intervals and equal weighting are used [16,17], so good agreement was expected. Uncertainty in σ resulted in a systematic error of less than 10% of the reported values. Fig. 2 shows results obtained from the simulations (solid gray lines indicating the mean and dashed gray lines one standard deviation above and below).

The simulations also show that the variation in D observed on cells cannot be explained on the basis of statistics, as the simulation includes localization uncertainty, finite track length, exposure time, and equal weight fitting. Thus, there is additional variation of *biological* origin.

We believe that receptor clusters originate from cell surface protrusions that form the initial contact points with the substrate [8]. The cluster is thus maintained (while it is maintained) by the cell morphology; this allows for the relatively free diffusion of receptors confined within it. It is intriguing that, while the majority (~70%) of receptors remain free to diffuse within the area of confinement, ~30% do show slow mobility – a slightly higher proportion than is found (using photobleaching recovery) among uncrosslinked receptors in resting cells [23]. Nonetheless, most receptors do remain highly mobile. As receptor-mediated signaling still occurs with fluid lipid membrane substrates [6,7], receptor immobilization does not appear to be a prerequisite for transmembrane signaling. We note also that other recent studies [9] have indicated clearly that receptor immobilization is not required for signaling.

3.3. IgE–FcεRI receptors can hop between clusters

Although receptors are generally confined, on rare occasions, a receptor can be observed to leave one cluster and enter a different cluster. Fig. 3 depicts a trajectory of such a cluster-hopping receptor. The color coding indicates the relative brightness of the receptor, with red being dimmest and blue brightest. During transit, the IgE–FcεRI appears to be farther from the substrate, as it is dimmer in TIRF. Thus, during transit this receptor is no longer in close proximity to the supported lipid bilayer; either the IgE must dissociate from the lipid-bound ligand, or the lipid-bound ligand must be extracted from the membrane. Although cells can easily develop sufficient force to extract phospholipids from membranes [26], we believe that this event involved ligand dissociation from IgE. Firstly, spontaneous IgE-DNP dissociation is rather fast (τ = 100 s [27]). Secondly, the trajectory of the receptor appears to be diffusive, not directed, as might be expected if the cell were exerting force on the receptor.

It is noteworthy that the IgE–FcεRI appeared to diffuse more rapidly when in transit in between clusters, comparable to observed IgE–FcεRI motion in central patches. This may indicate that the release of diffusional constraints over much of the cell surface is a precursor to the formation of the larger central patches and patch coalescence.

3.4. Slowly diffusing receptors are not influenced by receptor cluster motion

As previously mentioned ~30% of receptors in clusters are no more mobile than the clusters themselves. This raises the possibility that they are, in fact, *immobile* within the cluster, and their motion is simply the collective motion of the cluster. To address this hypothesis, we looked for correlation between the cluster and the single receptor hop directions. A histogram of receptor hop directions, relative to the cluster hop direction, is shown in Fig. 4 in a polar plot. The same number of correlated (251) and anticorrelated (258) hops was observed, within statistical variation. Thus, slowly diffusing receptors are not simply moving with the cluster as a whole. In fact, they do not even appear to be *influenced* by the cluster motion. This may indicate that the cytoskeletal elements responsible for maintaining cluster (contact) points do not move, but rather assemble and disassemble so as to produce contact zone movement.

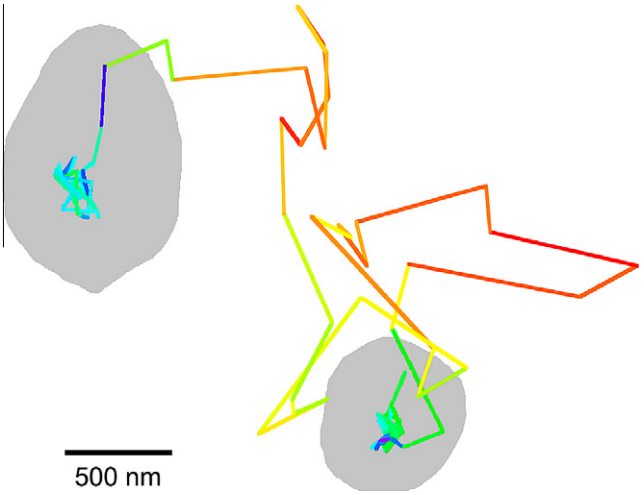

Fig. 3. Fluorescent IgE–FcεRI receptor (IgE–FcεRI) trajectory obtained from single-particle tracking at 20 frames/s. Total internal reflection fluorescence (TIRF) microscope images were collected ~30 s after initial cell–substrate contact. The color coding indicates the relative brightness of the IgE–FcεRI, with red being dimmest and blue brightest. The IgE–FcεRI is initially confined in the bottom left cluster (gray) and then transits to the top cluster. During transit, the receptor appears to be no longer in close proximity (dimmer in TIRF) to the supported lipid bilayer. Moreover, the IgE–FcεRI appears to diffuse (as determined from linear MSD plot) more rapidly (larger hops) when in transit between clusters, indicating release of diffusional constraints over the cell surface. Scale bar = 500 nm.

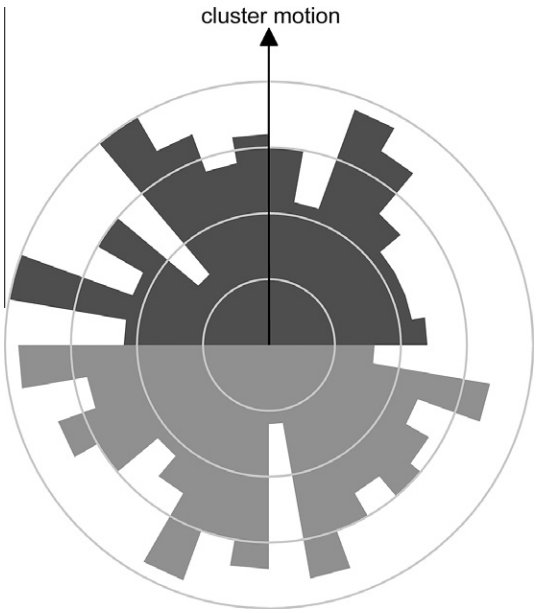

Fig. 4. Histogram in polar coordinates of IgE–FcεRI receptor complex (IgE–FcεRI) hop direction, relative to receptor cluster hop direction, which is represented by the arrow. Here, receptors were no more mobile than the clusters themselves and a total of 509 cluster–receptor vector pairs obtained from individual hops (every 50 ms) were analyzed (7 IgE–FcεRI and cluster trajectories). 251 IgE–FcεRI displacement vectors had a component in the direction of cluster motion (dark gray), and within statistical variation an equal number of 258 had a downward component (light gray). Thus, slowly diffusing receptors are not influenced by cluster motion and are mobile within the cluster.

4. Conclusions

This study presents what we believe to be the first quantitative evidence that anti-DNP IgE–FcεRI receptor complexes undergo relatively free diffusion within micron-sized receptor clusters. These clusters originate from cell surface protrusions that form initial contact points with a monovalent antigen-bearing fluid lipid bilayer; such bilayers are able to trigger mast cells via the IgE–FcεRI [6,7]. To directly observe IgE–FcεRI receptor motion within these contact points, we applied two-color TIRF microscopy together

with single-particle tracking and MSD analysis. To ensure the absence of bias in the fitting MSD plots, Monte Carlo simulations of diffusion tracks (with localization uncertainty) were fit by the same procedure.

The typical diffusion coefficient of liganded receptor in clusters was comparable to that of the monomeric, uncrosslinked IgE–FcεRI receptor on free cell surfaces [14]. Although about 30% of the receptors did diffuse slowly, their motion was uncorrelated with that of the micron-sized clusters in which they were located. In the central patches that result from coalescence of clusters, receptors diffused much faster, consistent with the apparent absence of actin cytoskeleton in the central region [7]. Hence RBL cell central patches may prove to be a useful model system to study protein diffusion in the absence of cytoskeletal interactions. On rare occasions, a receptor was observed to leave one cluster and enter a different cluster; the loss of confinement appears to be caused by IgE dissociation from its ligand. In between clusters, receptors showed very rapid diffusion (even before the central patches have formed), suggesting that the loss of diffusional constraints is actually a precursor to the formation of the large central patch. In conclusion, our results suggest at least three distinct states of receptor mobility in mast cells, and provide further evidence that receptor immobilization is not a prerequisite for signaling.

Acknowledgments

The authors thank Amanda Carroll-Portillo for helping with experimental protocols, Bridget Wilson for providing the RBL-2H3 mast cell line, and Jason Byars for conjugating anti-DNP IgE with fluorescent dyes. This work was supported in part by the Program in Interdisciplinary Biological and Biomedical Sciences funded by the University of New Mexico (to K.S.), award number T32EB009414 from the National Institute of Biomedical Imaging and Bioengineering, and by the UNM Spatiotemporal Modeling Center, award number P50GM085273 from the National Institutes of Health. The content is solely the responsibility of the authors and does not necessarily represent the official views of the National Institute of Biomedical Imaging and Bioengineering or the National Institutes of Health.

Appendix A. Supplementary data

Supplementary data associated with this article can be found, in the online version, at doi:10.1016/j.febslet.2012.01.013.

References

[1] Metzger, H. (1992) Transmembrane signaling: the joy of aggregation. J. Immunol. 149, 1477–1487.
[2] Galli, S.J., Tsai, M. and Piliponsky, A.M. (2008) The development of allergic inflammation. Nature 454, 445–454.
[3] Thomas, J.L., Feder, T.T. and Webb, W.W. (1992) Effects of protein concentration on IgE receptor mobility in rat basophilic leukemia cell plasma membranes. Biophys. J. 61, 1402–1412.
[4] Thomas, J.L., Holowka, D., Baird, B. and Webb, W.W. (1994) Large-scale co-aggregation of fluorescent lipid probes with cell surface proteins. J. Cell Biol. 125, 795–802.
[5] Posner, R.G., Subramanian, K., Goldstein, B., Thomas, J., Feder, T., Holowka, D. and Baird, B.A. (1995) Simultaneous cross-linking by two nontriggering bivalent ligands causes synergistic signaling of IgE FcεRI complexes. J. Immunol. 155, 3601–3609.
[6] Weis, R.M., Balakrishnan, K., Smith, B.A. and McConnell, H.M. (1982) Stimulation of fluorescence in a small contact region between rat basophil leukemia cells and planar lipid membrane targets by coherent evanescent radiation. J. Biol. Chem. 257, 6440–6445.
[7] Carroll-Portillo, A., Spendier, K., Pfeiffer, J., Griffiths, G., Li, H., Lidke, K.A., Oliver, J.M., Lidke, D.S., Thomas, J.L., Wilson, B.S. and Timlin, J.A. (2010) Formation of a mast cell synapse: FcεRI membrane dynamics upon binding mobile or immobilized ligands on surfaces. J. Immunol. 184, 1328–1338.
[8] Spendier, K., Carroll-Portillo, A., Lidke, K.A., Wilson, B.S., Timlin, J.A. and Thomas, J.L. (2010) Distribution and dynamics of rat basophilic leukemia immunoglobulin E receptors (FcεRI) on planar ligand-presenting surfaces. Biophys. J. 99, 388–397.
[9] Andrews, N.L., Pfeiffer, J., Martinez, M.A., Haaland, D.M., Davis, R.W., Kawakami, T., Oliver, J.M., Wilson, B.S. and Lidke, D.S. (2009) Small, mobile FcεRI aggregates are signaling competent. Immunity 31, 469–479.
[10] Liu, F.-T., Bohn, J.W., Ferry, E.L., Yamamoto, H., Molinaro, C.A., Sherman, L.A., Klinman, N.R. and Katz, David H. (1980) Monoclonal dinitrophenyl-specific murine IgE antibody: preparation, isolation, and characterization. J. Immunol. 124, 2728–2736.
[11] Seagrave, J., Pfeiffer, J.R., Wofsy, C. and Oliver, J.M. (1991) Relationship of IgE receptor topography to secretion in RBL-2H3 mast cells. J. Cell Physiol. 148, 139–151.
[12] Werner, J.H., Montano, G.A., Garcia, A.L., Zurek, N.A., Akhadov, E.A., Lopez, G.P. and Shreve, A.P. (2009) Formation and dynamics of supported phospholipid membranes on a periodic nanotextured substrate. Langmuir 25, 2986–2993.
[13] Hendriks, C.L.L., van Vliet, L.J., Rieger, B., van Kempen, G.M.P. and van Ginkel, M. (1999) Dipimage: a scientific image processing toolbox for MATLAB. Quantitative Imaging Group, Faculty of Applied Sciences, Delft University of Technology, Delft, The Netherlands.
[14] Andrews, N.L., Lidke, K.A., Pfeiffer, J.R., Burns, A.R., Wilson, B.S., Oliver, J.M. and Lidke, D.S. (2008) Actin restricts FcεRI diffusion and facilitates antigen-induced receptor immobilization. Nat. Cell Biol. 10, 955–963.
[15] Qian, H., Sheetz, M.P. and Elson, E.L. (1991) Single particle tracking: analysis of diffusion and flow in two-dimensional systems. Biophys. J. 60, 910–921.
[16] Saxton, M.J. (1997) Single-particle tracking: the distribution of diffusion coefficients. Biophys. J. 72, 1744–1753.
[17] Michalet, X. (2010) Mean square displacement analysis of single-particle trajectories with localization error: Brownian motion in an isotropic medium. Phys. Rev. E 82, 041914.
[18] Rieger, B., Dietrich, H.R.C., Van den Doel, L.R. and Van Vliet, L.J. (2004) Diffusion of microspheres in sealed and open microarrays. Microsc. Res. Tech. 65, 218–225.
[19] Saxton, M.J. and Jacobson, K. (1997) Single-particle tracking: applications to membrane dynamics. Annu. Rev. Biophys. Biomol. Struct. 23, 373–399.
[20] Saxton, M.J. (1995) Single-particle tracking: effect of corrals. Biophys. J. 69, 389–398.
[21] Savin, T. and Doyle, P.S. (2005) Static and dynamic errors in particle tracking microrheology. Biophys. J. 88, 623–638.
[22] Kusumi, A., Sako, Y. and Yamamoto, M. (1993) Confined lateral diffusion of membrane receptors as studied by single particle tracking (nanovid microscopy). Effects of calcium-induced differentiation in cultured epithelial cells. Biophys. J. 65, 2021–2040.
[23] Wade, W.F., Freed, J.H. and Edidin, M. (1989) Translational diffusion of class II major histocompatibility complex molecules is constrained by their cytoplasmic domains. J. Cell Biol. 109, 3325–3331.
[24] Menon, A.K., Holowka, D., Webb, W.W. and Baird, B. (1986) Cross-linking of receptor-bound IgE to aggregates larger than dimers leads to rapid immobilization. J. Cell Biol. 102, 541–550.
[25] Lidke, D.S., Andrews, N.L., Pfeiffer, J.R., Jones, H.D.T., Sinclair, M.B., Haaland, D.M., Burns, A.R., Wilson, B.S., Oliver, J.M. and Lidke, K.A. (2007) Exploring membrane protein dynamics by multicolor single quantum dot imaging using wide field, TIRF, and hyperspectral microscopy. Proc. SPIE 6448, 64480Y.
[26] Evans, E. (2001) Probing the relation between force-lifetime-and chemistry in single molecular bonds. Annu. Rev. Biophys. Biomol. Struct. 30, 105–128.
[27] Xu, K., Goldstein, B., Holowka, D. and Baird, B. (1998) Kinetics of multivalent antigen DNP-BSA binding to IgE–FcεRI in relationship to the stimulated tyrosine phosphorylation of FcεRI. J. Immunol. 160, 3225–3235.